

Validation for Solar Wind and CME Prediction

Lan Jian

NASA Goddard Space Flight Center, MD

9th CCMC Workshop

College Park, MD, USA

April 24, 2018

I. Validation for Solar Wind Prediction

Collaborators: P. MacNeice, M. L. Mays,
A. Taktakishvili, D. Odstrcil, B. Jackson,
P. Riley, I. V. Sokolov

Thanks to NSF Award AGS-1242798

Widely-Used Coronal and Heliospheric Models Installed at the CCMC

GONG: Global Oscillation Network Group

NSO/SOLIS: National Solar Observatory at Kitt Peak,

Synoptic Optical Long-term Investigations of the Sun

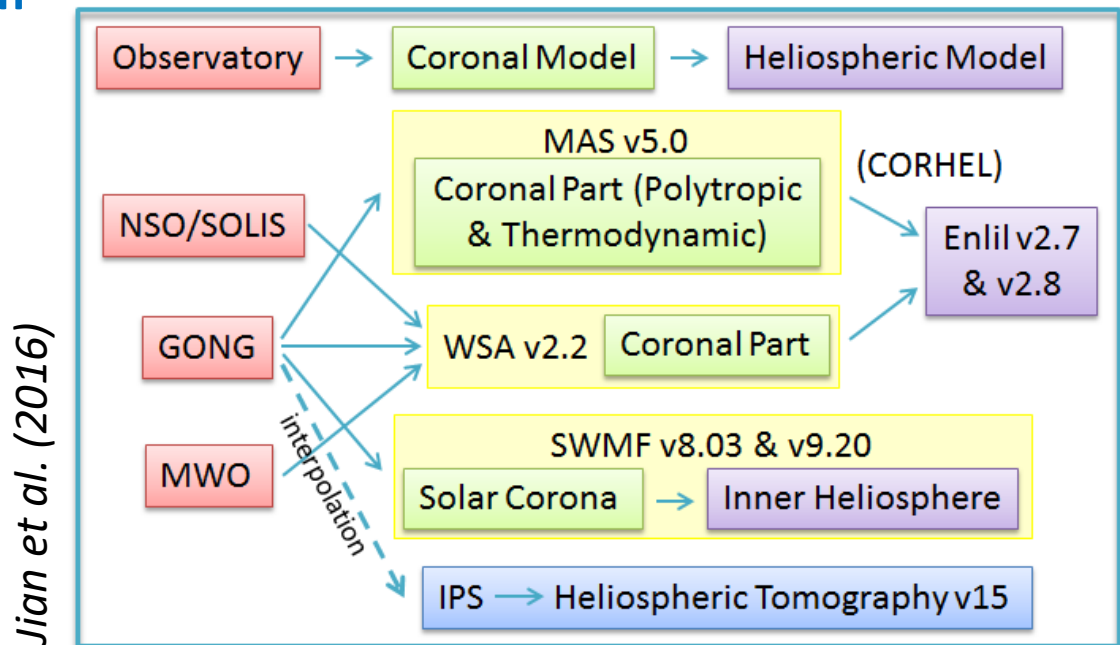
MWO: Mount Wilson Observatory

MAS: MHD-Around-a-Sphere model

WSA: Wang-Sheeley-Arge model

SWMF: Space Weather Modeling Framework

IPS: Interplanetary Scintillation



Introduction of the Model Description, Resolution, and Inner Boundary Condition

Model	Description			Resolution		Inner Boundary Condition
WSA v2.2 coronal part, up to 21.5 R_s	PFSS+Schatten current sheet model, semiempirical			Magnetogram with a smoothed resolution of 2.5° in latitude and longitude	101×92×182 (radial × latitude × longitude) → (0.20 R_s , 2.0°, 2.0°)	Radial surface field, magnitude is set so that its line of sight component matches magnetogram
MAS v5.0 coronal part, up to 30 R_s	3-D MHD model	Polytropic	Zero beta approximation	Magnetogram with a resolution of 1° in latitude and longitude	101×101×128 → (0.29 R_s , 1.8°, 2.8°)	Base of corona: $T = 1.8$ MK and $N = 2 \times 10^8 \text{ cm}^{-3}$
		Thermodynamic	Full thermodynamic energy equation		151×101×182 → (0.19 R_s , 1.8°, 2.0°)	Chromosphere: $T = 0.02$ MK and $N = 2 \times 10^{12} \text{ cm}^{-3}$
Enlil heliospheric model, up to 430 R_s	3-D MHD model for super-Alfvénic solar wind, driven by WSA, MAS, and possible by other models too, only one temperature			v2.8, coupling with WSA	1024×120×360 → (0.40 R_s , 1.0°, 1.0°)	21.5 R_s : $V_{\text{slow}} = 200$ km/s, $V_{\text{fast}} = 700$ km/s, $T = 2$ MK, and $N = 200 \text{ cm}^{-3}$
				v2.7, coupling with MAS	320×60×180 → (1.25 R_s , 2.0°, 2.0°)	30 R_s : $V_{\text{slow}} = 250$ km/s, $V_{\text{fast}} = 650$ km/s, $T = 0.6$ MK, and $N = 150 \text{ cm}^{-3}$
SWMF, 3-D MHD model, up to 500 R_s , separate ion and electron temperatures	v8.03	Starting from corona, semiempirical solar wind heating		Nonuniform grid. Within 24 R_s : cell size ranging 0.025-0.75 R_s . Heliospheric part (starting at 20 R_s): a minimum cell size of 1 R_s	Top of chromosphere: $T = 0.02$ MK and $N = 2 \times 10^{10} \text{ cm}^{-3}$	
	v9.20	Starting from the upper chromosphere, adding physics-based turbulent Alfvén wave dissipation for coronal heating and solar wind acceleration		Non-uniform grid. Inside 1.7 R_s : the angular resolution of 1.4°. Coronal part (chromosphere to 24 R_s): cell size ranging 0.001-0.8 R_s . Heliospheric part: 2 R_s within the current sheet and 8 R_s elsewhere (higher resolution of 1 R_s within the current sheet in a new refinement which is in progress)	Top of chromosphere: $T = 0.05$ MK and $N = 2 \times 10^{11} \text{ cm}^{-3}$	
IPS tomography v15	3-D reconstruction using a kinematic solar wind model and tomographically fitting it to IPS observation			Time cadence of 6 h (can be increased to 3 h after using more worldwide IPS data)	N/A	

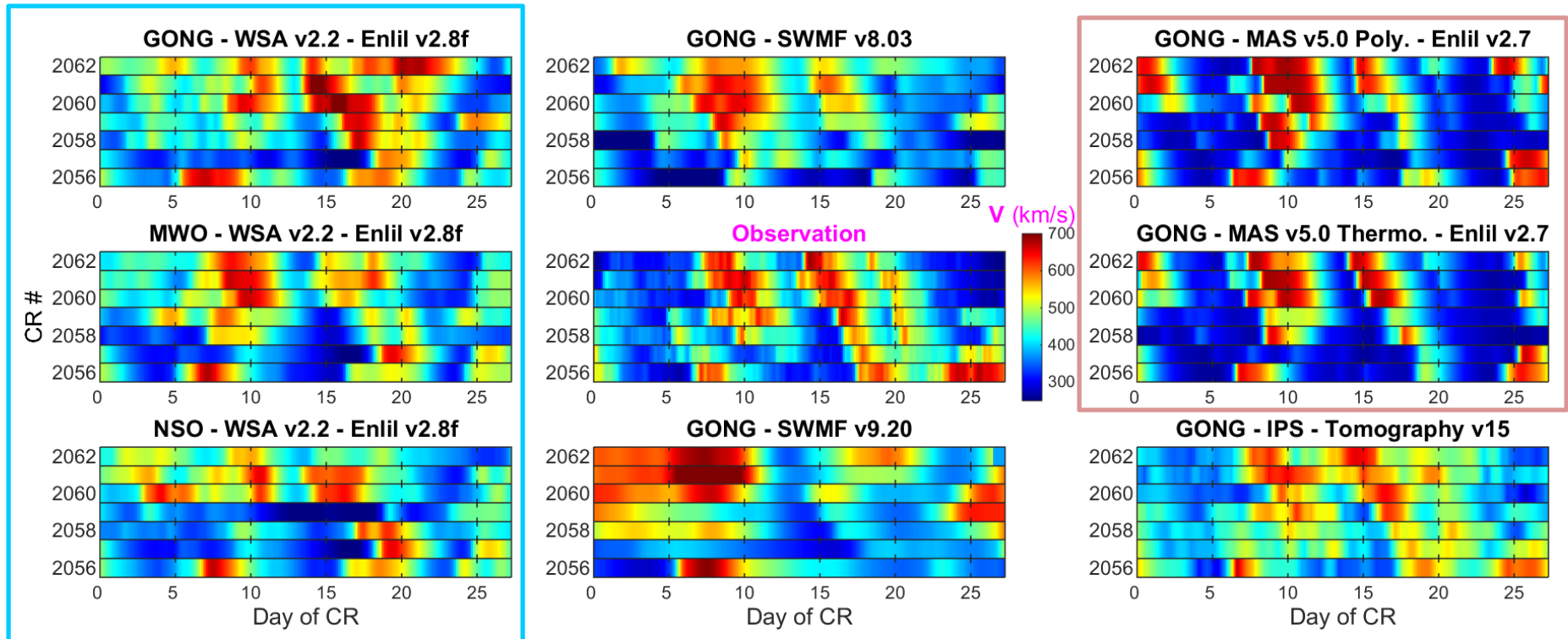
Performance Metrics for Solar Wind Simulation

Jian et al. (Space Weather, 2015, 2016) provided sample performance metrics using four parameters (V, B, N, T)

1. Visual comparison
2. Mean square error for time series of solar wind parameters (without & with normalization)
3. Model/observation ratio
4. Correlation between model and observation
5. Capturing IMF sectors (automatic identification of sectors)
6. Capturing slow-to-fast stream interaction regions (SIRs) (automatic identification of SIRs)
7. Capturing the latitudinal variations of solar wind
8. Statistics of solar wind at low latitudes and mid-to-high latitudes

Ulysses {

Comparison of Solar Wind Speed at Earth Orbit in 2007

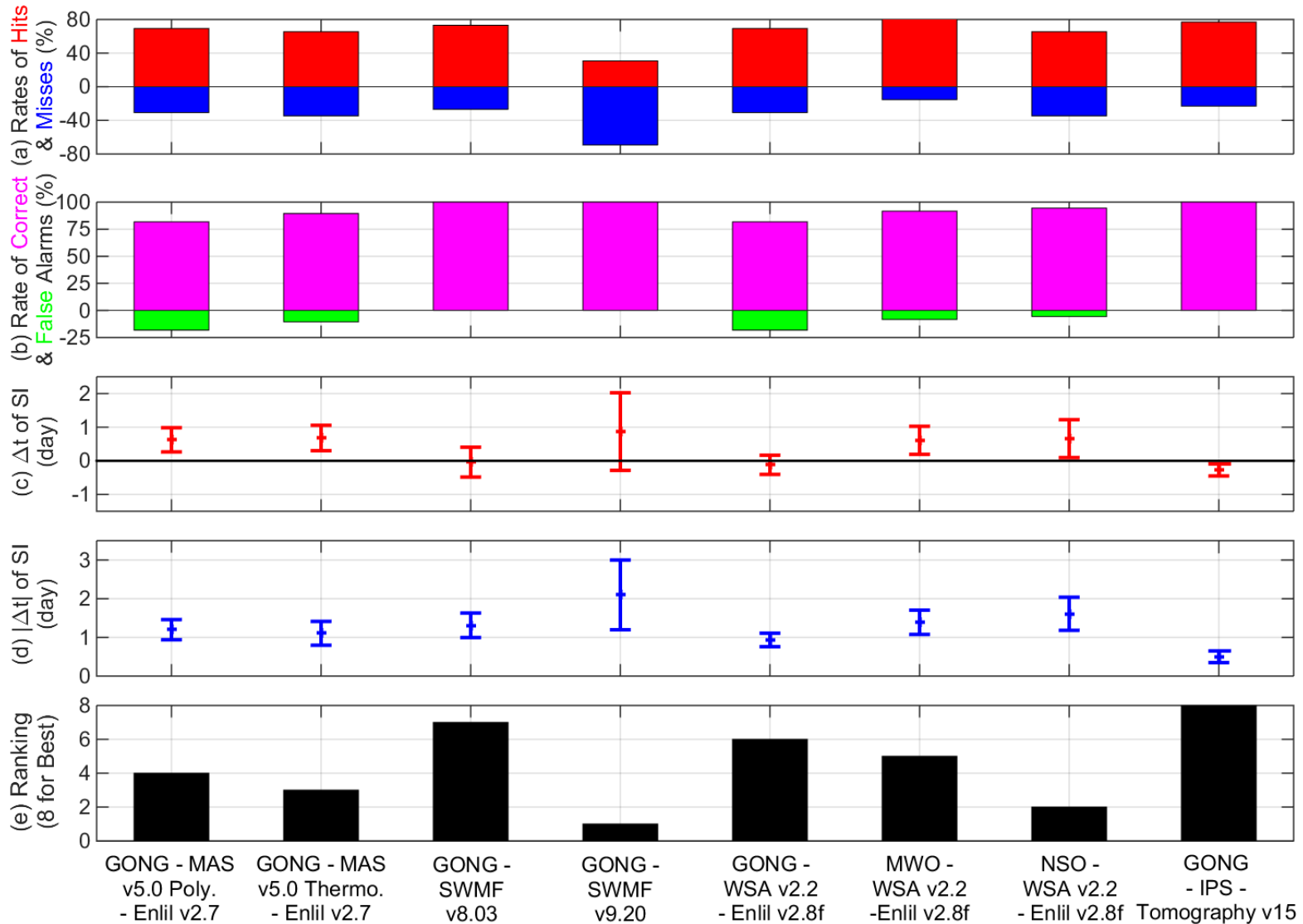


After Jian et al. (2015)

Large variability from the simulation results

- WSA v2.2 – Enlil v2.8 model using magnetograms from different sources
- Multiple models using the same GONG magnetogram
- Different versions of SWMF perform very differently

Capabilities of Capturing SIRs

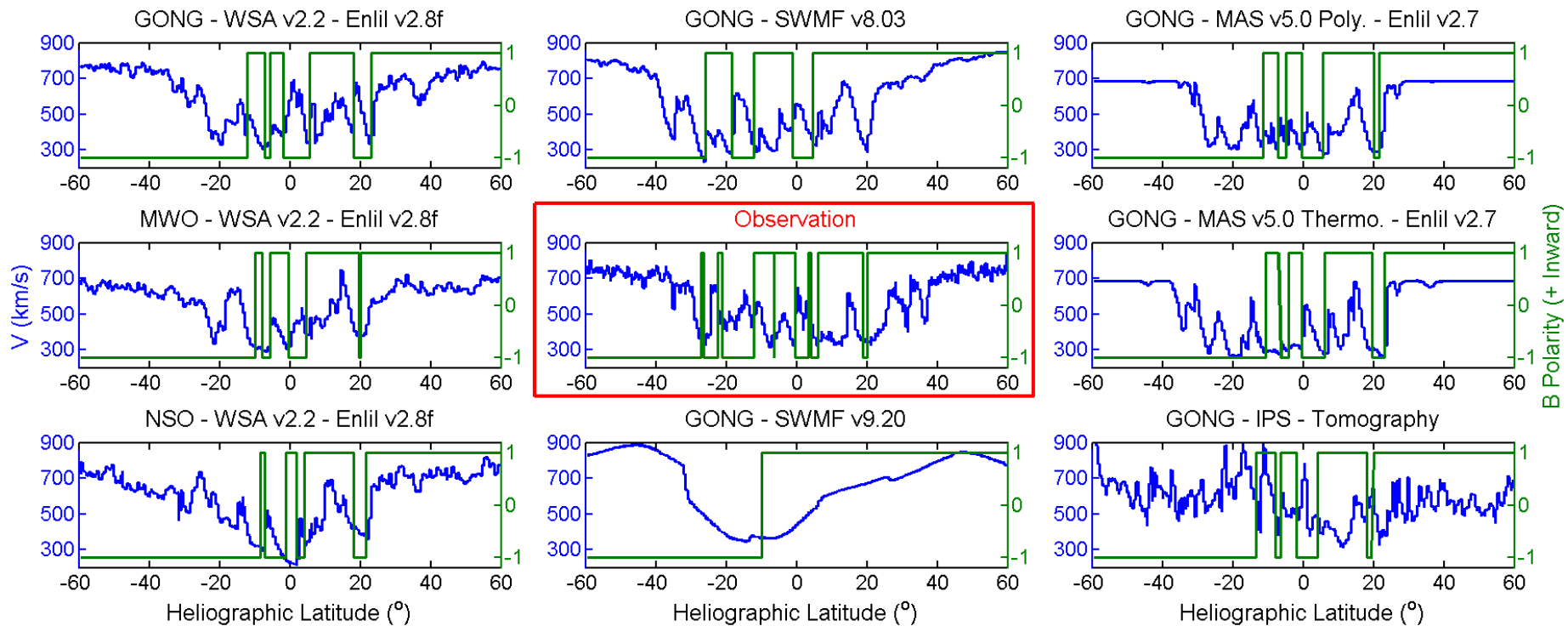


After Jian et al. (2015)



Capabilities of Capturing Latitudinal Variations of Solar Wind

Solar Wind Speed & IMF Polarity

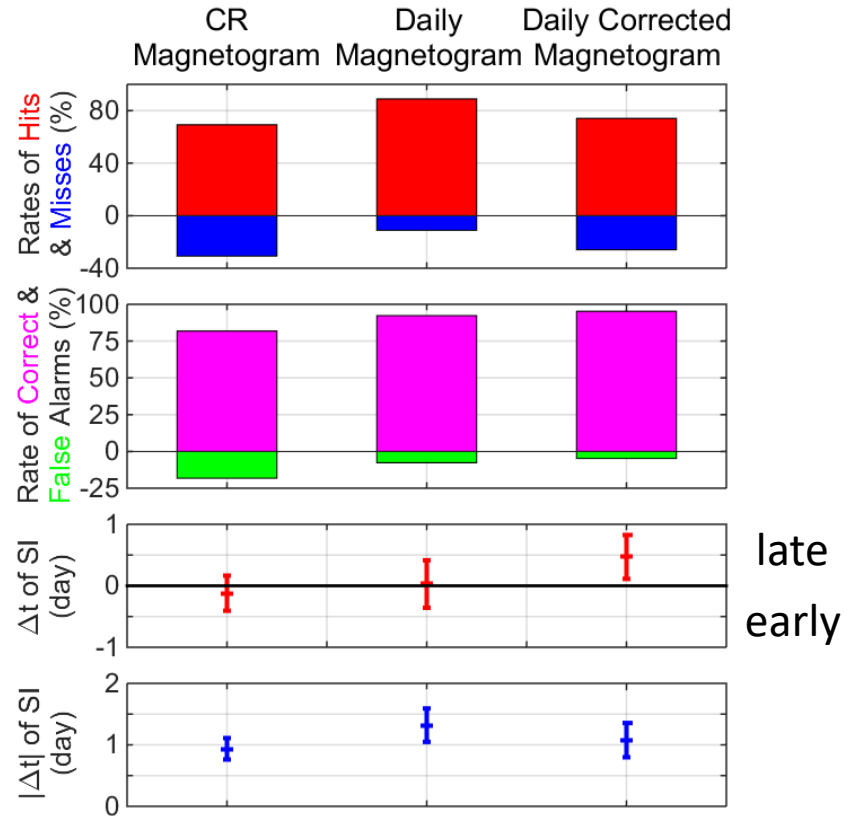
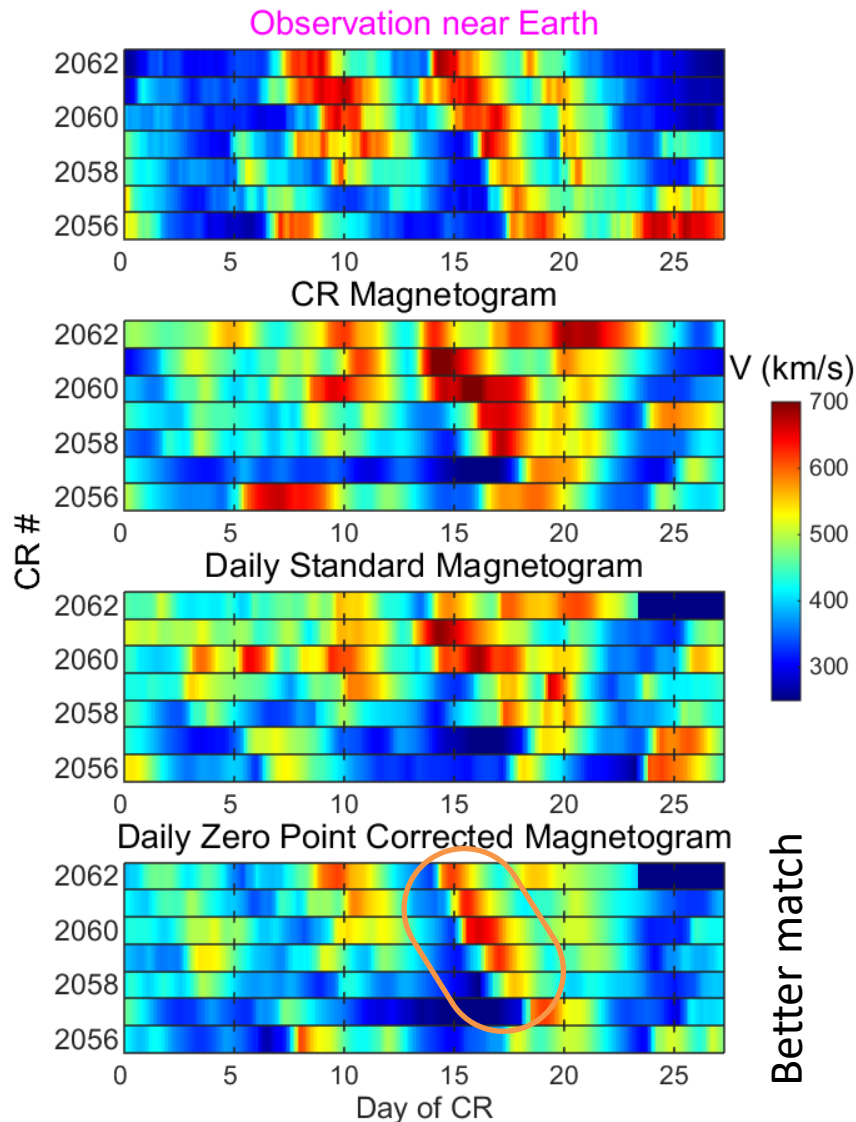


Jian et al. (2016)

Summary of the Model Evaluation for 2007

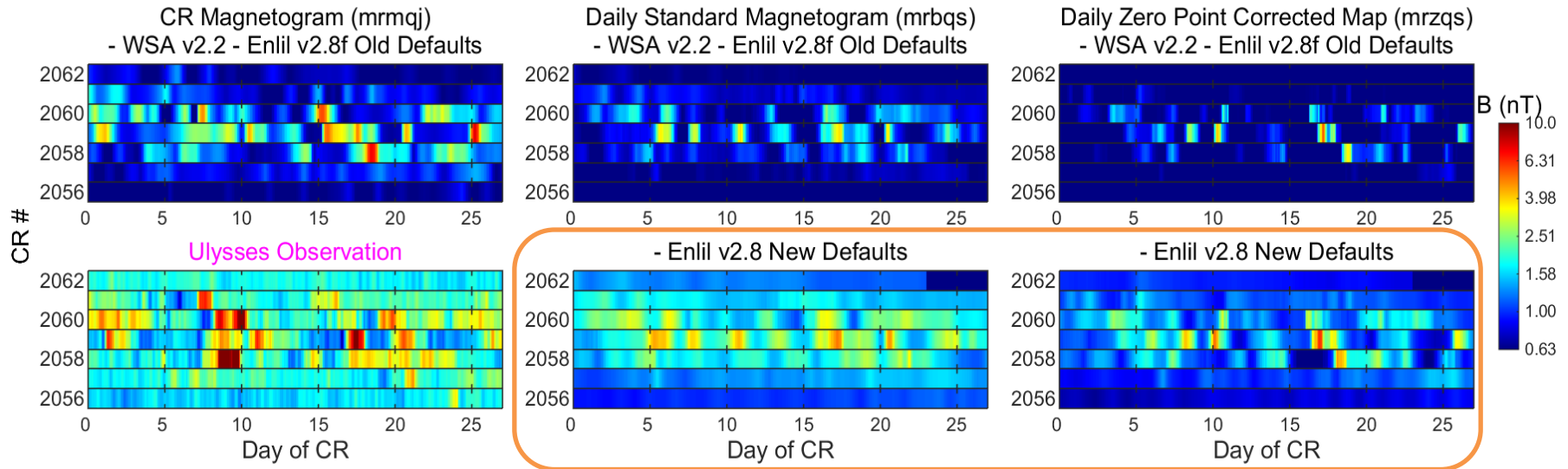
Synoptic Map	Model		Strength			Weakness	
	Solar Corona Part	Inner Heliospheric Part					
MWO	WSA v2.2	Enlil v2.8	lowest RMSE for N_p and B	match well with median B at all latitudes	match well with median N_p at all latitudes	underestimate the fast wind V at middle to high latitudes	
NSO/SOLIS			best match for low-latitude median B and T_p and high-latitude median V			largest RMSE for normalized V , second least correlation with V	
GONG	MAS v5.0 Polytropic	Enlil v2.7	second highest correlation for V		N/A		underestimate B at all latitudes
			lowest RMSE for V , normalized V , N_p , and T_p ; highest correlation for N_p , B , and T_p	highest correlation for V	N/A	underestimate the fast wind V at middle to high latitudes; overestimate low-latitude median N_p	
	second lowest RMSE for normalized V ; second highest correlation for N_p , B , and T_p	overestimate low-latitude median N_p most, underestimate low-latitude median B and T_p most					
	SWMF v8.03		match low-latitude median V best		largest RMSE for N_p , normalized N_p , B , and T_p ; lowest correlation for B and T_p		
	SWMF v9.20		capture the high-latitude hot solar wind well; lowest RMSE for T_p and normalized B		latitudinal variations are much smoothed; produce north-south asymmetry not observed by Ulysses; largest RMSE for V		
IPS Tomography v15		N/A		produce transient structures not observed by Ulysses at middle to high latitudes; could not capture the latitudinal variation of N_p ; lowest correlation for V and N_p ; mismatch high-latitude median V and N_p most			

WSA v2.2 – Enlil v2.8 Using Different Magnetogram Synoptic Maps from GONG



Riley et al. (2014) showed the conversion factor between different observatories can be > 10 , and it varies with latitude

WSA v2.2 – Enlil v2.8 Using Different GONG Magnetograms and Different Parameter Settings



Jian et al. (2016)

- **More than 10 parameters** are used in setting the ambient wind conditions at ENLIL's inner boundary
- They have been recently added in the WSA-Enlil result page as the **control file**
- The new setting has recently been implemented at CCMC

II. Validation of CME Prediction Using WSA-Enlil+Cone Model

Collaborators: D. Odstrcil, M. L. Mays

Thanks to NSF Award AGS-1321493

Introduction of the Modeling System

- ❖ The WSA-Enlil model uses kinematic properties of CMEs inferred from coronal and/or heliospheric observations to launch a CME-like **hydrodynamic** structure at **21.5 Rs** (Arge and Pizzo, 2000; Arge et al., 2004; Odstrcil et al., 2005)
- ❖ The Enlil model at CCMC has been gradually evolving for run-on-request, but it has been kept as **v2.7** for the predictions at NOAA/SWPC
- ❖ Main new features used in the present **v2.9** of Enlil model
 - Using a sequence of the WSA maps computed from the closest GONG daily synoptic magnetogram
 - Self-correcting model free parameters based on monthly-averaged in situ measurements at 1 AU
 - More reliable identification of disturbances by multi-grid computations
 - Revised the volumetric heating that is independent on the numerical time step variations
 - Enhanced visualization, synthetic white-light images, and input for SEP model and IPS tomography

CME Parameters Used as Model Input

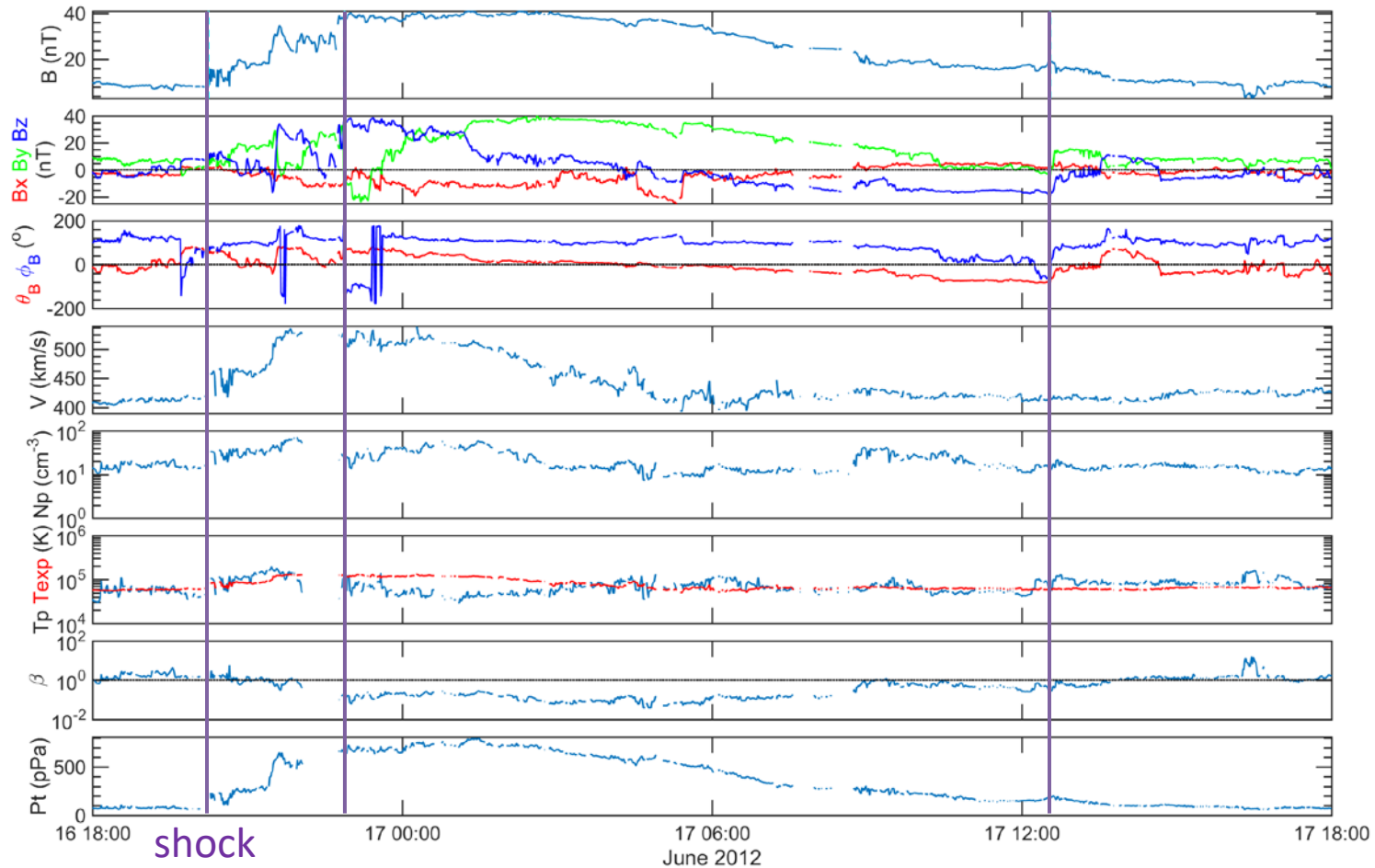
Cone	date lat lon radcld vcld dcld tcld	Leading edge at 21.5 Rs at this time (yyyy-mm-ddThh:mm) Heliographic latitude of the cone axis (deg) Heliographic longitude of the cone axis (deg) Half-width of the cone (deg) Velocity of the cone (km/s) Density of the cone as factor of mean stream value Temperature of the cone as factor mean stream value
Cavity if radcav > 0	radcav dcav tcav	Radius of the cavity as factor of radcld Density of the cavity as factor of mean stream value Temperature of the cavity as factor of mean stream value

- The geometrical CME properties are approximated by the Cone model
- At CCMC, CME parameters are determined using
 - Stereoscopic CME Analysis Tool (StereoCAT) based on tracking specific CME features (Pulkkinen et al., 2010)
 - **Since about 2014**, CME Analysis Tool (CAT) to capture the volumetric structure of CMEs (Pizzo and Biesecker, 2004; Millward et al., 2013)
- The CME parameters and simulation graphic outputs since 2010 → CCMC/DONKI
- The Enlil simulation results including graphic outputs in 2007-2016 at **Helioweather**
- The simulations use a **medium** spherical grid size of 512×60×180 (r, θ , ϕ) to cover 0.1-2.1 AU in radius, $\pm 60^\circ$ in latitude, and 360° in longitude
- Output is of ~4-min cadence at Earth

Recent History of Our Validation Effort

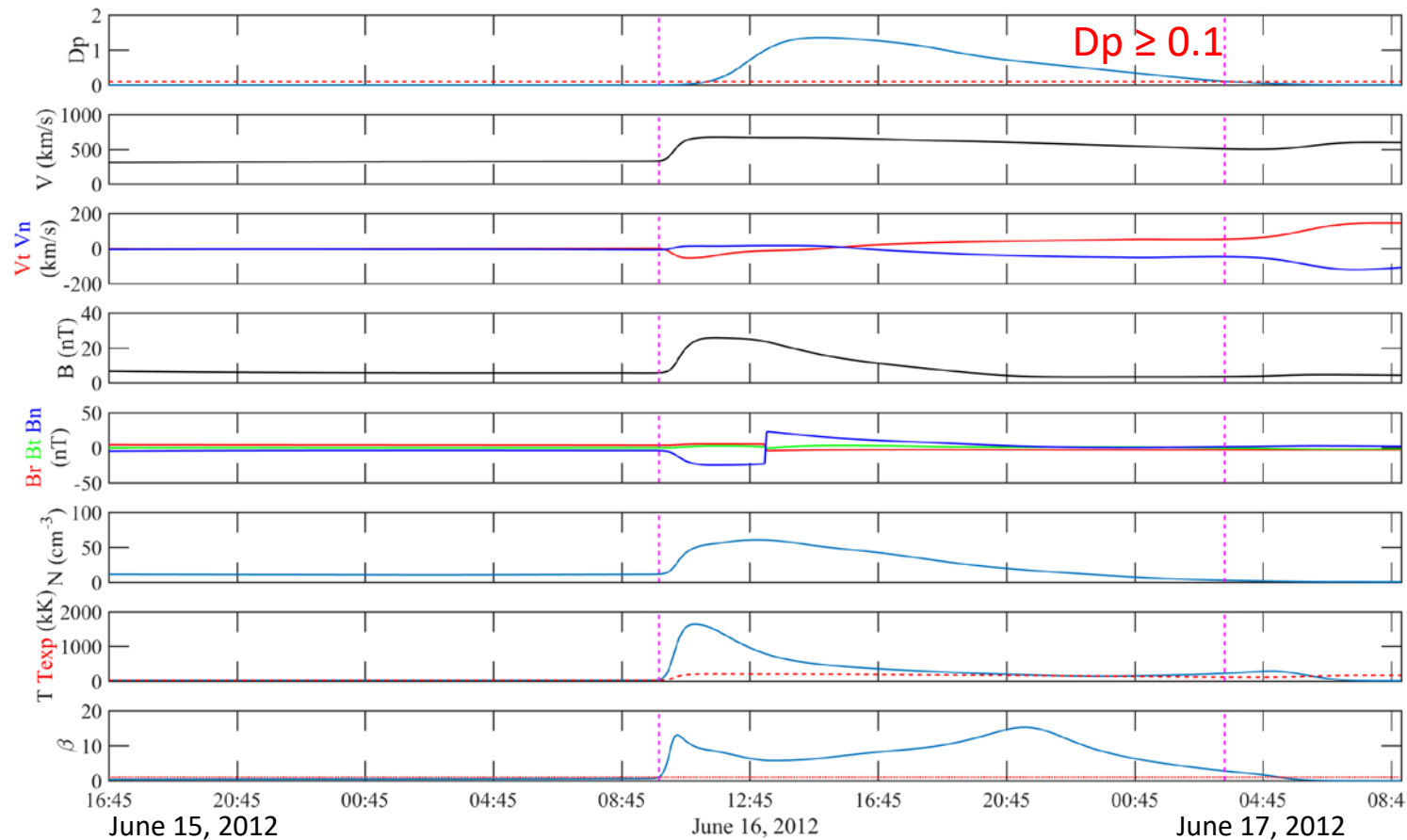
- 2016
 - CMEs in 2012-2015
 - CME input from CCMC/SWRC
- 2017
 - CMEs with an initial speed > 400 km/s in 2007-2016
 - CME input from the **fixed-phi** fitting (angular width = 60°) from the joint Heliospheric Cataloguing, Analysis and Techniques Service (HELICATS) project
- 2018
 - CMEs in 2010-2016
 - CME input from CCMC/SWRC (most are from **real-time prediction**)
 - Use GONG daily zero point corrected synoptic magnetograms
 - Self-correcting model free parameters based on monthly-averaged in situ measurements at 1 AU

A Survey of Interplanetary CMEs (ICMEs)



- **ICMEs = Magnetic Clouds (MCs) + ICMEs without well-defined flux ropes**
- Multiple (not all) criteria are used: increased magnetic field, field rotations over a large scale, lower than expected proton temperature, low β , bidirectional suprathermal electron strahls, speed decrease, increase of total pressure (Pt), etc.
- ICMEs at L1 are surveyed using 1-min OMNI data for 2010-2016. The ICME/MC catalogs from Richardson and Cane, Nieves-Chinchil, Wu and Lepping are used as references

Identification of Simulated ICMEs



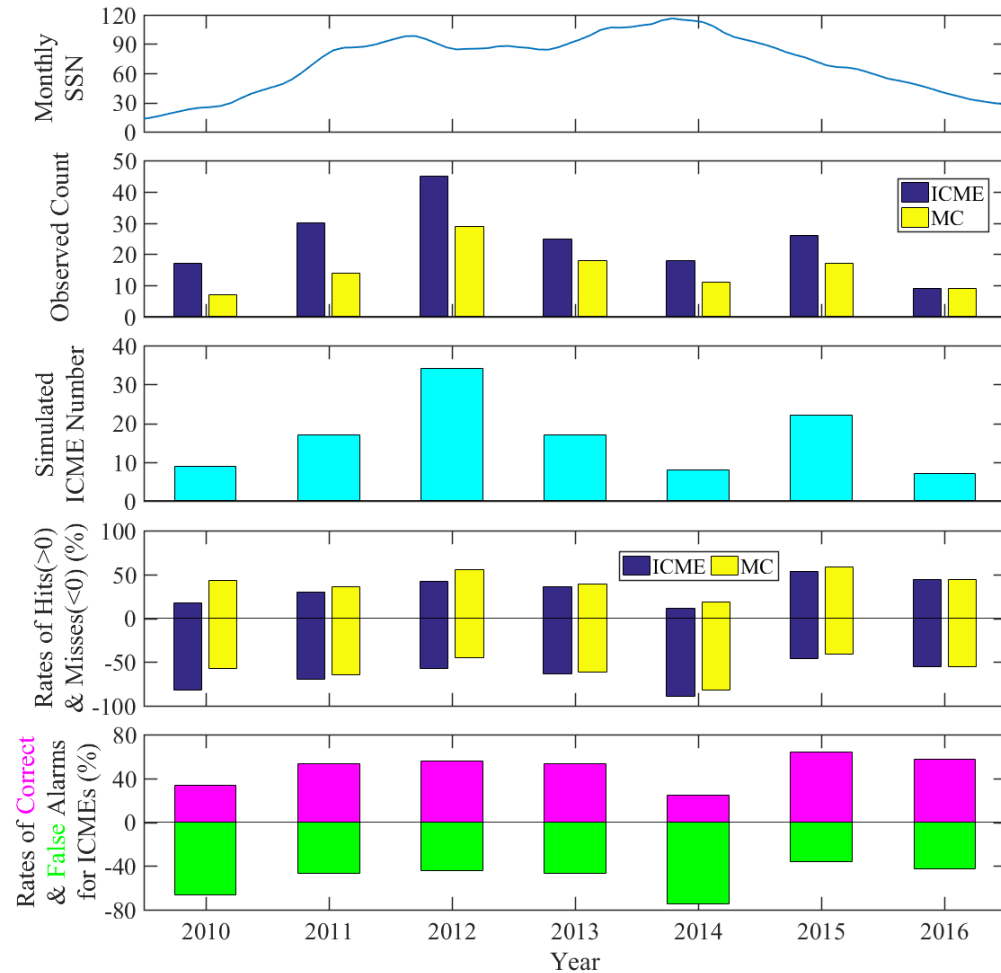
- ICMEs in simulations are identified by requiring $D_p \geq 0.1$
- ICME start time
 - The closest time when V and/or B increases sharply, earlier than $D_p \geq 0.1$
 - If there is no sharp increase of V or B , choose the time when V and/or B starts to increase
- ICME end time: at the end time of $D_p \geq 0.1$ or when solar wind parameters return to ambient, whichever comes last

Statistics of ICME Prediction in 2010-2016

	Observed	Captured	Rate of Hits (%)	Rate of Misses (%)	Simulated	Rate of Correct Alarms (%)	Rate of False Alarms (%)	Absoulte Offset of Arrival Time (hr)
ICMEs	170	60	35.3	64.7	114	52.6	47.4	11.5±1.4
MCs	105	47	44.8	55.2	N/A	N/A	N/A	13.4±1.8
ICMEs with shock	99	46	46.5	53.5	N/A	N/A	N/A	9.2±1.2

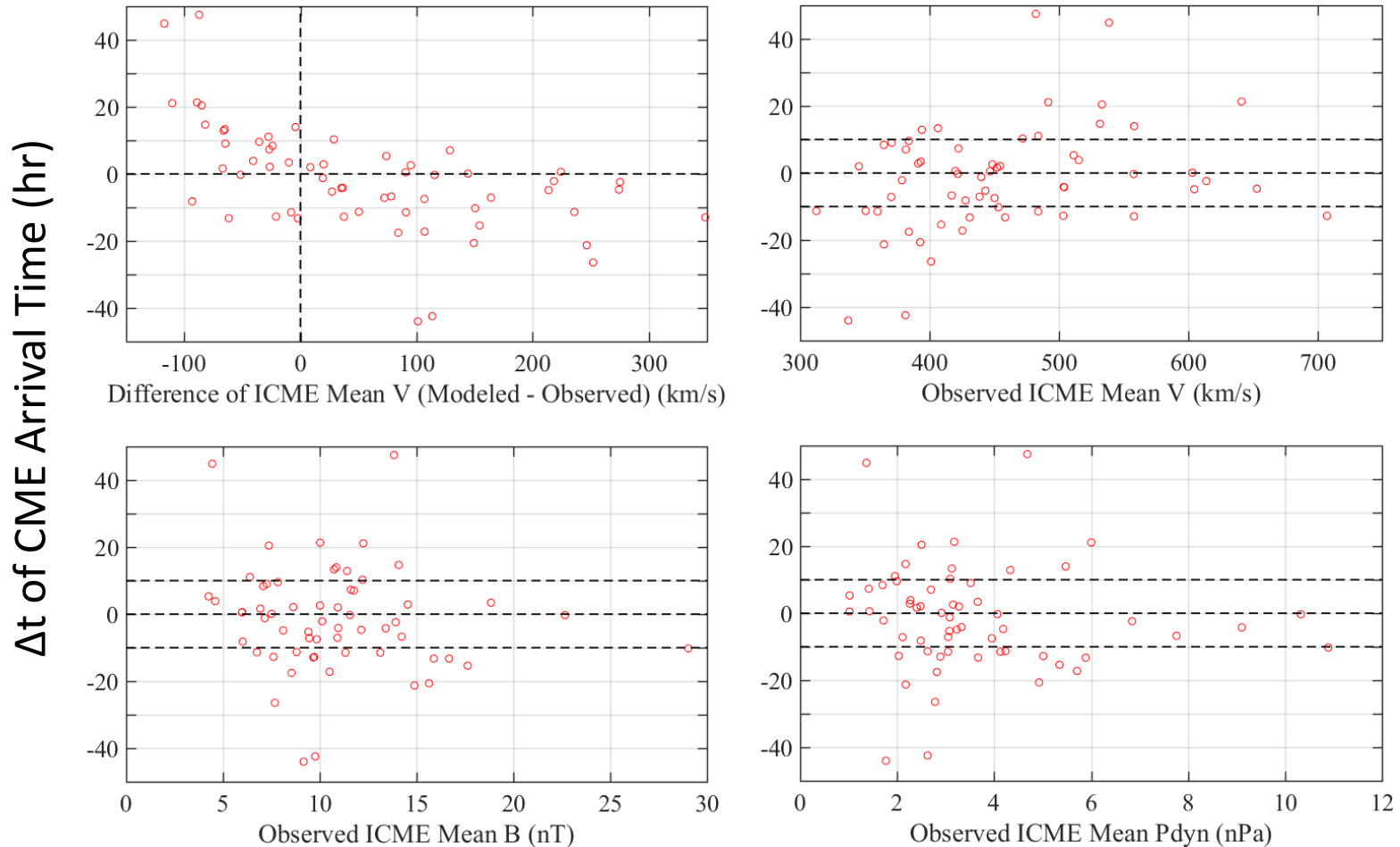
- At Earth, 114 ICMEs are identified in the simulation data
- If there are shocks, shock time is used as the ICME start time
- A slight preference (55%) of early arrival
- For the same CME, the arrival time from the Enlil simulation with different settings can readily differ by 6 hours or more

Annual Variations of ICME Prediction



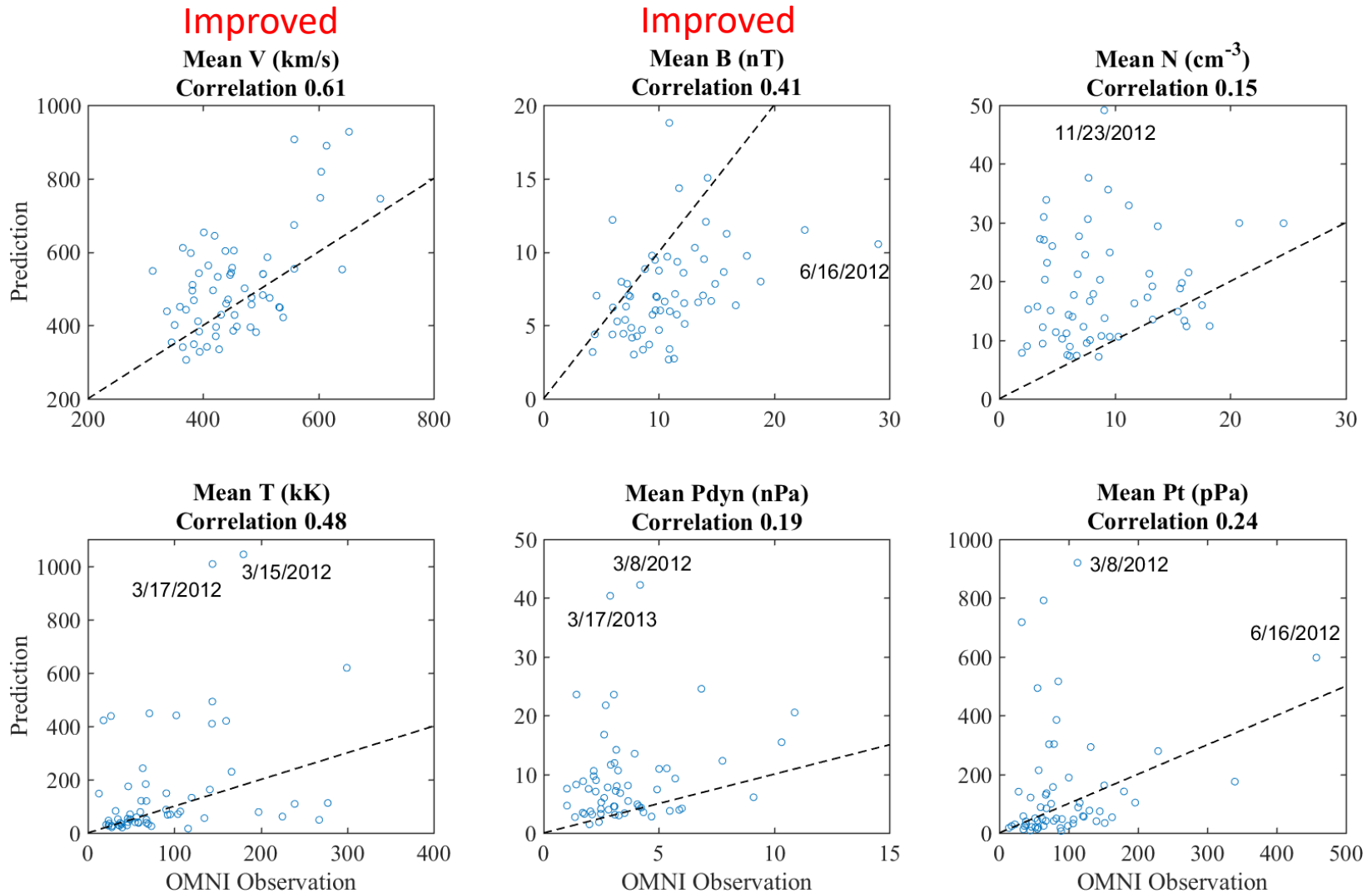
- The performance of CME prediction varies much from year to year
- The rates of hits and correct alarms drop in 2014, possibly related to the change of the CME fitting methods at CCMC and the less help from STEREO remote observations

Factors Affecting the ICME Arrival Time



- ✓ As expected, the faster the predicted ICME speed than the observed speed, the earlier the ICME arrives at 1 AU than observed
- ✓ For **faster and stronger ICMEs**, their arrival time is generally better predicted

Simulated vs. Observed Mean Parameters of ICMEs



Summary and Discussion

- Comprehensive performance metrics are developed for solar wind prediction and are easy to adapt
- The inter-comparison of the models can be affected by their different grids, internal parameter settings, and inner boundary conditions
- The WSA-Enlil+Cone model is validated for long-term CME prediction. The results depend much on the model version and CME input parameter
- Statistically the prediction of the arrival time, ICME speed and magnetic field is improved but there is drawback in some other aspects
- We need to validate the modeling of a small number of CMEs which are well observed remotely and in situ. Well-calibrated CME parameters are highly needed!
- We need to include **internal magnetic field structures** in the Enlil model